

Turbulent Flow and Large Surface Wave Events in the Marine Boundary Layers

Peter P. Sullivan

National Center for Atmospheric Research

Boulder, CO 80307-3000

Phone:(303) 497-8953 fax:(303) 497-8171 email: pps@ucar.edu

James C. McWilliams

Department of Atmospheric Sciences and

Institute of Geophysics and Planetary Physics, UCLA

Los Angeles, CA 90095-1565

Phone:(310) 206-2829 fax:(310) 206-5219 email: jcm@atmos.ucla.edu

Grant Number: N00014-07-M-0516

LONG-TERM GOALS

The long term objective of our research for the “High Resolution Air-Sea Interaction” (HIRES) Departmental Research Initiative (DRI) is to identify the couplings between large wave events, winds, and currents in the surface layer of the marine boundary layers. Turbulence resolving large eddy simulations (LESs) and direct numerical simulations (DNSs) of the marine atmospheric boundary layer (MABL) in the presence of time and space varying wave fields will be the main tools used to elucidate wind-wave-current interactions. A suite of turbulence simulations over realistic seas using idealized and observed pressure gradients will be carried out to compliment the field observations collected in moderate to high winds. The database of simulations will be used to generate statistical moments, interrogated for coherent structures, and ultimately used to compare with HIRES observations.

OBJECTIVES

Our goals are: 1) participate in the planning process for the HIRES field campaign; and 2) construct and exercise an LES code applicable to the HIRES high wind regime.

APPROACH

We are investigating interactions between the MABL and the connecting air-sea interface primarily using LES. The waves are externally imposed based on well established empirical wave spectra. Ultimately they will be provided by direct observations of the sea surface from the HIRES field campaign. The main technical advance is the development of a computational tool that allows for nearly arbitrary 3-D wave fields, *i.e.*, the sea surface elevation $h = h(x, y, t)$ as a surface boundary condition. The computational method allows for time and space varying surface conditions over a range of wave scales $\mathcal{O}(10)$ m or larger as shown below.

WORK COMPLETED

Meetings: We attended a PI meeting in La Jolla, CA that focused on a first preliminary look at the observational datasets collected during the HIRES field campaign conducted in June 2010.

Simulations: Here we briefly describe a process study that examines the combined influence of wave age and convection on MABL dynamics. Often the wind driven MABL is either cooled or heated at the surface and thus it is of interest to consider flow over waves in the presence of atmospheric stability. Previously, we examined the impact of stratification using DNS (Sullivan & McWilliams, 2002) and LES (Sullivan *et al.*, 2008) over an idealized monochromatic wave. The current process study builds on our previous work with neutrally stratified flows and we vary the geostrophic wind from $U_g = [5 - 20]$ m s⁻¹ and add a small amount of unstable convective forcing at the water surface, $Q_* = 0.01$ K m s⁻¹ ~ 10 W m⁻². The computational domain is $(X_L, Y_L, Z_L) = (1200, 1200, 800)$ m and is discretized using $(N_x, N_y, N_z) = (512, 512, 128)$ gridpoints. A broadband wave spectrum is considered. The virtual surface wave field is built to match a Pierson and Moskowitz (1964) wave spectrum with random phases with a directional spectrum picked to emphasize long crested waves. The wave field is built based on the assumption of a surface wind speed of 15 m s⁻¹ and then the phase speed of the peak in the wave spectrum $C_p \sim 18$ m s⁻¹. An $x - y$ view of the 3D surface wave field at a particular instant in time is given in figure 1. Further details of the LES experimental design are provided in our FY 2010 progress report. Table 1 lists bulk properties of the past and current simulations, *viz.*, the geostrophic wind, wave age $\mathcal{A} = C_p/U_{10}$, friction velocity u_* , surface heat flux Q_* , Monin-Obukhov stability index L , and reference wind speed at $z = 10$ m, *i.e.*, U_{10} . The height of the MABL in these simulations is $z_i \sim 500$ m and thus the Deardorff (1972) convective scale $w_* \sim 0.53$ m s⁻¹. Consequently, simulations (without wave effects) are in a mixed shear-convective regime that tend to develop broad streamwise rolls (*e.g.*, Moeng & Sullivan, 1994). In addition to the simulations with a wavy lower boundary we also consider a run *ACF* with a flat lower boundary as a reference for run *AC*. A description of the code and first results are described in Sullivan *et al.*(2010a). We note that the algorithmic formulation is general and also allows turbulence simulations over and around 3D stationary orography as described in Sullivan *et al.*(2010b) ¹.

RESULTS

Large eddy simulations and also observations find that surface waves impact the mean winds, vertical momentum fluxes, and turbulence variances depending on the wave state (or wave age) and the wind-wave orientation. We are particularly interested in changes in vertical momentum flux $u'w'$ when a broadband wave spectrum is imposed at the lower boundary for neutral and unstable stratification.

In Figure 2 we show contours of instantaneous resolved momentum flux $\overline{u'w'}/u_*^2$ for simulations of *neutrally* stratified flow with the same surface wave spectrum at two wind speeds $U_g = [5, 20]$ m s⁻¹. The impact of waves on the turbulence in the surface layer is dramatic. In the high wave age (low wind) case we clearly observe high amplitude momentum flux correlated

¹The meeting papers Sullivan *et al.*, (2010a,b) are available at <http://www.mmm.ucar.edu/people/sullivan/>.

Table 1: Simulation properties

Run	U_g (m s ⁻¹)	$\mathcal{A} = C_p/U_{10}$	u_* (m s ⁻¹)	Q_* (K m s ⁻¹)	L
<i>A</i>	5	4.8	0.124	0.0	∞
<i>AC</i>	5	4.8	0.166	0.01	-35.0
<i>ACF</i>	5	–	0.167	0.01	-35.6
<i>B</i>	7.5	3.4	0.187	0.0	∞
<i>C</i>	10	2.8	0.228	0.0	∞
<i>D</i>	15	1.9	0.338	0.0	∞
<i>E</i>	20	1.5	0.452	0.0	∞
<i>EC</i>	20	1.5	0.539	0.01	-1200.0

with the underlying wave field. Both positive and negative pockets extend in the y direction and these patches are observed to move with the propagating wave field. The fluctuations are large compared to the mean flux, the ratio can be greater than 10. In contrast the simulation with strong winds (wind-wave equilibrium) generates flux structures that are elongated in the stream-wise direction (see right panel of Figure 2). Hints of the underlying wave field can be detected under close inspection of the image. Notice also the instantaneous fluctuations are also greatly reduced compared to the low wind simulation.

The distribution of momentum flux by quadrants for neutrally stratified flow is presented in the upper panels of Figure 3. The decomposition is by quadrants: $Q^I(\bar{u}' > 0, \bar{w}' > 0)$, $Q^{II}(\bar{u}' < 0, \bar{w}' > 0)$, $Q^{III}(\bar{u}' < 0, \bar{w}' < 0)$, and $Q^{IV}(\bar{u}' > 0, \bar{w}' < 0)$. The flux patterns in Figures 2 and 3 are fundamentally tied to the movement of the underlying surface. The differences between the low wind (high wave age) and high wind (low wave age) cases is a reflection of the competition between irrotational “wave pumping” and rotational turbulence. Surface waves generate a near irrotational flow field that contributes momentum flux in the positive signed quadrants [Q^I, Q^{III}]. Turbulence on the other hand mainly contributes to the negative signed quadrants [Q^{II}, Q^{IV}]. The competition between wave pumping and turbulence is nearly in balance for flow over swell with the net momentum flux slightly negative. At higher winds, *i.e.*, closer to wind-wave equilibrium, turbulence increases in magnitude and overwhelms the motions induced by wave pumping leading to a momentum flux primarily tilted into quadrants [Q^{II}, Q^{IV}]. At high winds the majority of the surface wave modes are traveling slower than the surface winds and hence tend to act similar to surface roughness. As a result of swell, surface layer fluxes and mean winds are altered compared to their counterparts over stationary rough surfaces.

Wave pumping is also active when surface heating is added as an external forcing. The lower panel of Figure 3 compares the quadrant flux distribution for slightly heated simulations over a spectrum of waves and a flat stationary surface. Again the fast moving surface waves add significant contributions to the positive signed quadrants [Q^I, Q^{III}] that nearly balances the negative signed momentum fluxes in quadrants [Q^{II}, Q^{IV}]. The lower right panel of Figure 3 further illustrates that the momentum flux over a stationary rough surface is at least qualitatively similar to turbulent flow in wind-wave equilibrium.

In the simulations with surface heating and high wave age, the static pressure fluctuations depicted in Figure 4 exhibit a structure clearly tied to the underlying wave field which is markedly different than in the case of a flat lower boundary; this is analogous to what was observed in

neutral flow. There is an ongoing debate as to the vertical influence of surface waves with the majority of the studies concluding that the “wave boundary layer” is shallow $\mathcal{O}(10\text{ m})$ or much less (*e.g.*, Mastenbroek *et al.*1996). Most often these investigations consider neutral flow and $\mathcal{A} < 1$. In Figure 5 we compare second and third order moments of vertical velocity $\langle \overline{w^2} \rangle / u_*^2$ and $\langle \overline{w^3} \rangle / u_*^3$ for one of our mixed shear-convective simulations. As expected the vertical velocity variance shows a pronounced near surface maximum because of the rapid propagation of surface waves. The elevated maximum near the middle of the MABL is also found in numerous simulations and observations of highly convective boundary layers. This is caused by the presence of coherent thermal structures. The third order moment, which has a maximum near the middle of the boundary layer $\sim 250\text{ m}$, is noticeably reduced in the presence of swell compared to a heated stationary surface. The third order moment of w is related to vertical transport of turbulent kinetic energy, $\sim -\partial \langle \overline{w^3} \rangle / \partial z$, and the reduction hints that surface waves have altered the important coherent structures that develop near the surface. This is a topic for future exploration with LES over a wider range of stability.

IMPACT/APPLICATIONS

The computational tools developed and the database of numerical solutions generated will aid in the interpretation of the observations gathered during the past HIRES field campaign. In addition idealized process studies performed with the simulations have the potential to improve our understanding of the mechanisms that lead to surface drag under high wind conditions.

TRANSITIONS & RELATED PROJECTS

The current work is a collaborative effort between NCAR, numerous university investigators and international research laboratories. Also the present work has links to the ONR DRI on the impact of typhoons in the Western Pacific Ocean (ITOP).

REFERENCES

- Deardorff, J. W., 1972: Numerical investigation of neutral and unstable planetary boundary layers. *Journal of the Atmospheric Sciences*, **29**, 91-115.
- Mastenbroek, C., V. K. Makin, M. H. Garat & J. P. Giovanangeli, Experimental evidence of the rapid distortion of turbulence in the air flow over water waves. *Journal of Fluid Mechanics*, **318**, 273-302.
- Moeng, C.-H. & P. P. Sullivan, 1994: A comparison of shear and buoyancy driven planetary-boundary-layer flows. *Journal of the Atmospheric Sciences*, **51**, 999-1022.
- Pierson, W. J. & L. Moskowitz, 1964: A proposed spectral form for fully developed wind seas based on the similarity theory of S. A. Kitaigorodskii. *Journal of Geophysical Research*, **69**, 5181-5190.
- Sullivan, P. P. & J. C. McWilliams, 2002: Turbulent flow over water waves in the presence of stratification. *Physics of Fluids*, **14**, 1182-1195.

Sullivan, P. P., J. B. Edson, T. Hristov, & J. C. McWilliams, 2008: Large eddy simulations and observations of atmospheric marine boundary layers above non-equilibrium surface waves. *Journal of the Atmospheric Sciences*, **65**, 1225-1245.

Sullivan, P.P., 2010a: Large eddy simulation of high wind marine boundary layers above a spectrum of resolved moving waves. *19th Symposium on Boundary Layers and Turbulence*, Keystone, CO.

Sullivan, P.P., E. G. Patton & K. W. Ayotte, 2010b: Turbulent flow over and around sinusoidal bumps, hills, gaps and craters derived from large eddy simulations. *19th Symposium on Boundary Layers and Turbulence*, Keystone, CO.

PUBLICATIONS

Sullivan, P. P. & E. G. Patton, 2011: The effect of mesh resolution on convective boundary layer statistics and structures generated by large-eddy simulation. *Journal of the Atmospheric Sciences*, [in press].

Weil, J. C., P.P. Sullivan, E. G. Patton & C-H. Moeng, 2011: Statistical variability of dispersion in the convective boundary layer: LPDM-LES model ensembles and observations. *Boundary-Layer Meteorology*, [submitted].

Nilsson, E. O., A. Rutgersson & P. P. Sullivan, 2011: Convective boundary layer structure in the presence of wind-following swell. *Quarterly Journal of the Royal Meteorological Society*, [submitted].

Van Roekle, L. P., B. Fox-Kemper, P. P. Sullivan, P. E. Hamlington & S. R. Haney, 2011: The form and orientation of Langmuir cells for misaligned winds and waves. *Journal of Geophysical Research*, [submitted].

Hanley, K. E., S. E. Belcher & P. P. Sullivan, 2011: Response to “Comments on a global climatology of wind-wave interaction”. *Journal of Physical Oceanography*, [in press].

Moeng, C.-H. and P.P. Sullivan 2011: Large Eddy Simulation. Encyclopedia of Atmospheric Sciences 2nd Edition, Eds. G. North, F. Zhang and J. Pyle. Academic Press, [submitted].

Liang, J., J. C. McWilliams, P. P. Sullivan & B. Baschek, 2011: Modeling bubbles and dissolved gases in the ocean. *Journal of Geophysical Research – Oceans*. **116**, C03015, 1-17.

Kukulka, T., A. J. Plueddemann, J. H. Trowbridge, & P. P. Sullivan, 2011: The influence of crosswind tidal currents on Langmuir circulation in a shallow ocean. *Journal of Geophysical Research – Oceans*, **116**, C08005, 1-15.

Lenschow, D. H., M. Lothon, S. D. Mayor, P. P. Sullivan, & G. Canut, 2011: A comparison of higher-order vertical velocity moments in the convective boundary layer from lidar with in situ measurements and LES. *Boundary-Layer Meteorology*, [in press].

Suzuki, N., T. Hara, & P. P. Sullivan, 2011: Turbulent airflow at young sea states with frequent wave breaking events: Large eddy simulation. *Journal of the Atmospheric Sciences*, **68**, 1290-1305.

Patton, E. T. Horst, P. Sullivan, D. Lenschow, S. Oncley, W. Brown, S. Burns, A. Guenther, A. Held, T. Karl, S. Mayor, L. Rizzo, S. Spuler, J. Sun, A. Turnipseed, E. Allwine, S. Edburg, B. Lamb, R. Avissar, R. Calhoun, J. Kleissl, W. Massman, K. Paw-U, & J. Weil, 2011: The canopy horizontal array turbulence study (CHATS). *Bulletin of the American Meteorological Society*, **92**, 593-611.

- Moeng, C.-H. Moeng, P. P. Sullivan, M. F. Khairoutdinov, & D. A. Randall, 2010: A mixed scheme for subgrid-scale fluxes in cloud-resolving models. *Journal of the Atmospheric Sciences*, **67**, 3692-3705.
- Sullivan, P. P. and E. G. Patton, 2011: Offshore marine boundary-layer winds predicted by a large eddy simulation model with resolved surface waves. *6th Theoretical Fluid Mechanics Conference*, American Institute of Aeronautics and Astronautics, Honolulu, HI.
- Nguyen, K. X. S. P. Oncley, T. W. Horst, P. P. Sullivan & C. Tong, 2010: Investigation of subgrid-scale turbulence in the atmospheric surface layer using AHATS field data. *American Physical Society, Fluid Dynamics*, Long Beach, CA.
- Suzuki, N., T. Hara, & P. P. Sullivan, 2010: Turbulent airflow at young sea states with frequent wave breaking events: Large eddy simulation. *17th Conference on Air Sea Interaction*, Annapolis, MD.
- Liang, J., J. C. McWilliams, P. P. Sullivan, 2010: Modeling gas bubbles in the ocean boundary layer. *17th Conference on Air Sea Interaction*, Annapolis, MD.

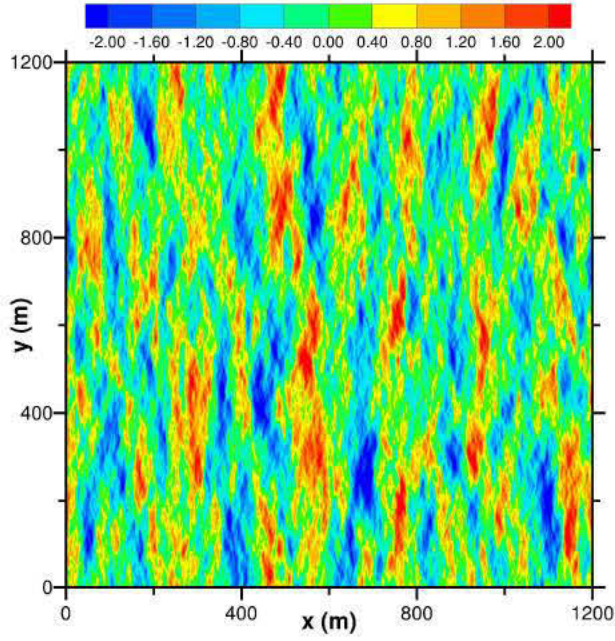


Figure 1: A snapshot of the instantaneous wave field height $h(x, y, t)$ that is imposed at the bottom of the LES code. h is built from a sum of linear plane waves, and waves propagate left to right according to the dispersion relationship. The horizontal grid spacing matches the LES, *i.e.*, $\Delta x = \Delta y = 2.34$ m. The color bar is in units of meters.

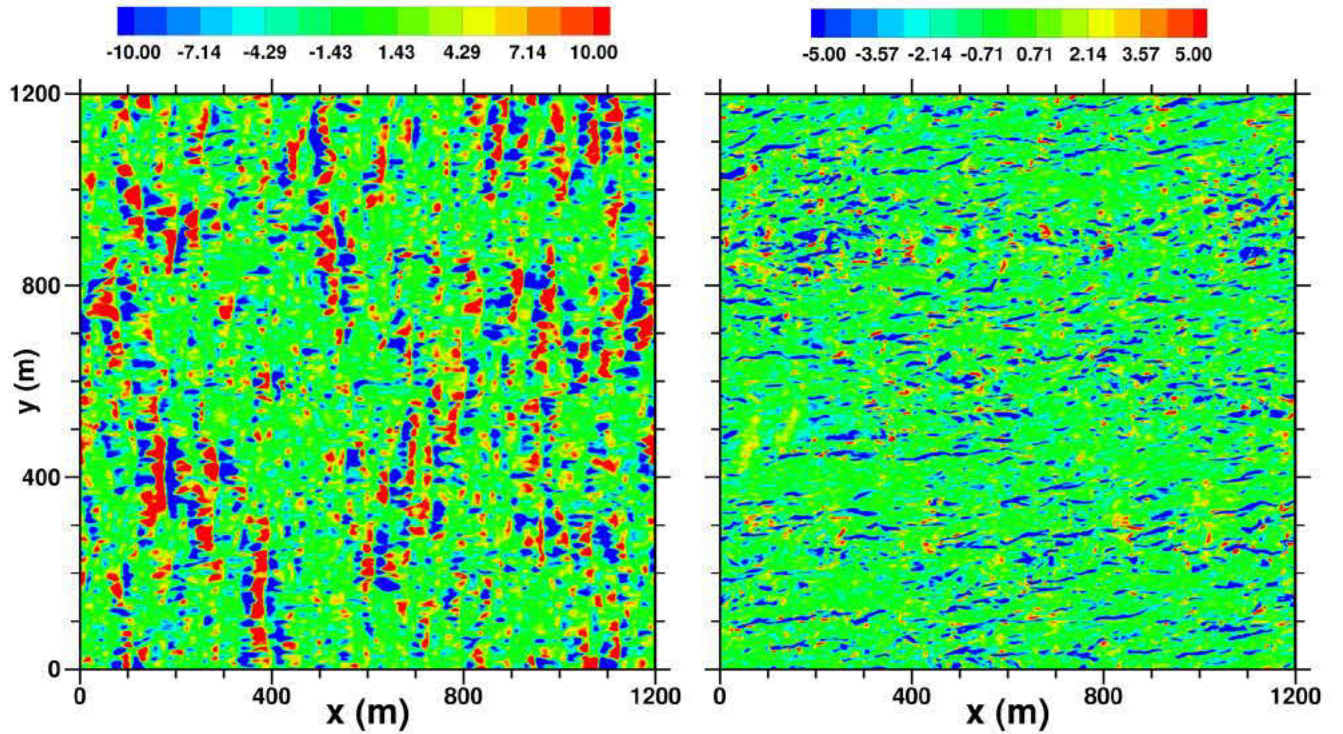


Figure 2: Resolved vertical momentum flux $u'w'/u_*^2$ in a wave following x - y plane near the water surface $\zeta = 5.8$ m. The left panel is a swell dominated regime with wave age ~ 4.8 ($U_g = 5 \text{ m s}^{-1}$) while the right panel is a case near wind-wave equilibrium with wave age ~ 1.4 ($U_g = 20 \text{ m s}^{-1}$). The wave spectrum at the bottom of the simulations is the same. Notice the range of the color bar is different between the two cases. The normalized fluctuations in the wind-wave equilibrium case are smaller.

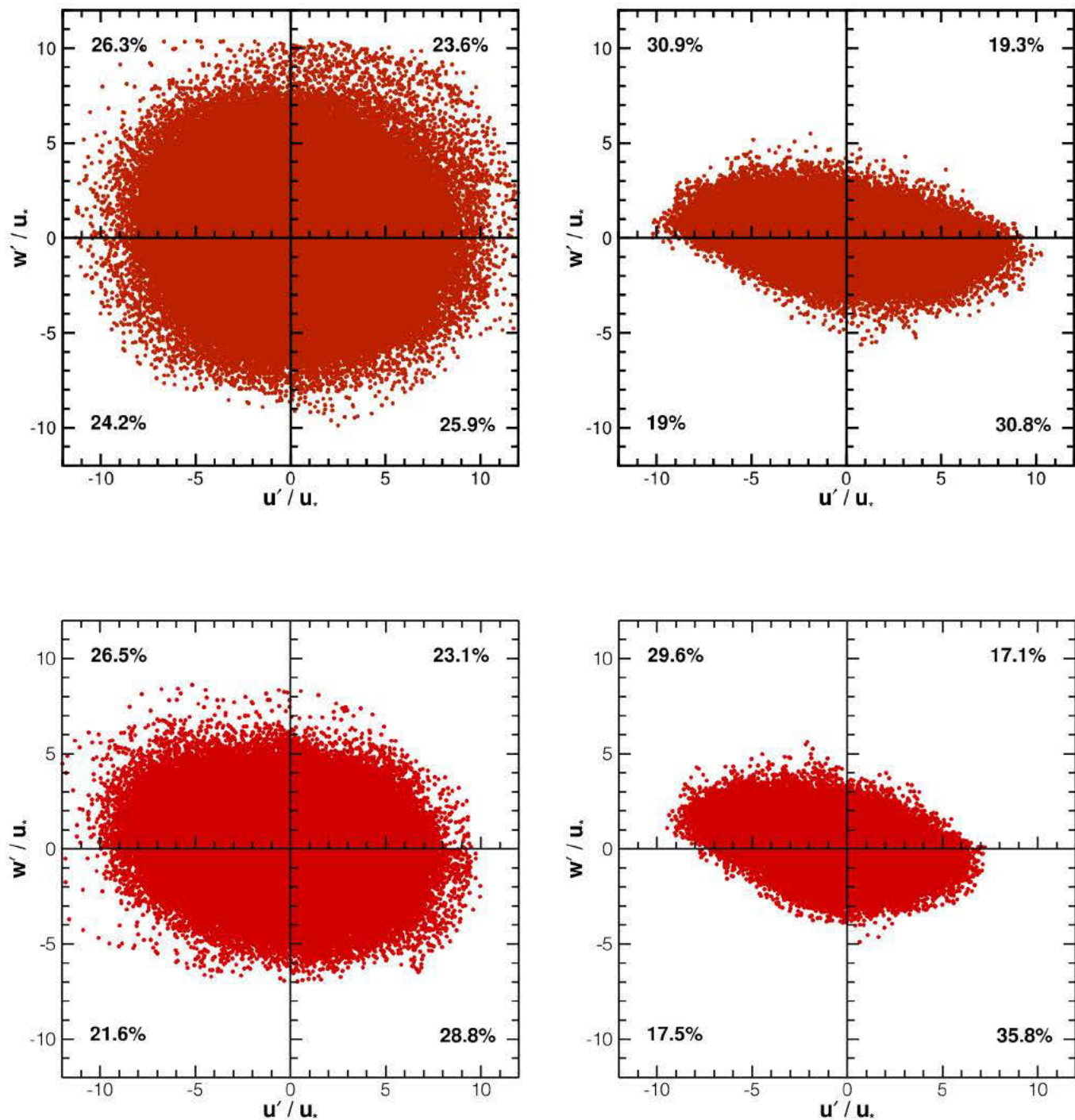


Figure 3: Quadrant analysis of vertical momentum flux. Upper left panel neutral flow over swell and upper right panel neutral flow over equilibrium wind waves. Lower left panel shear-convective flow over swell and lower right panel shear-convective flow over a flat surface (no waves). Each figure lists the fraction of points in each quadrant.

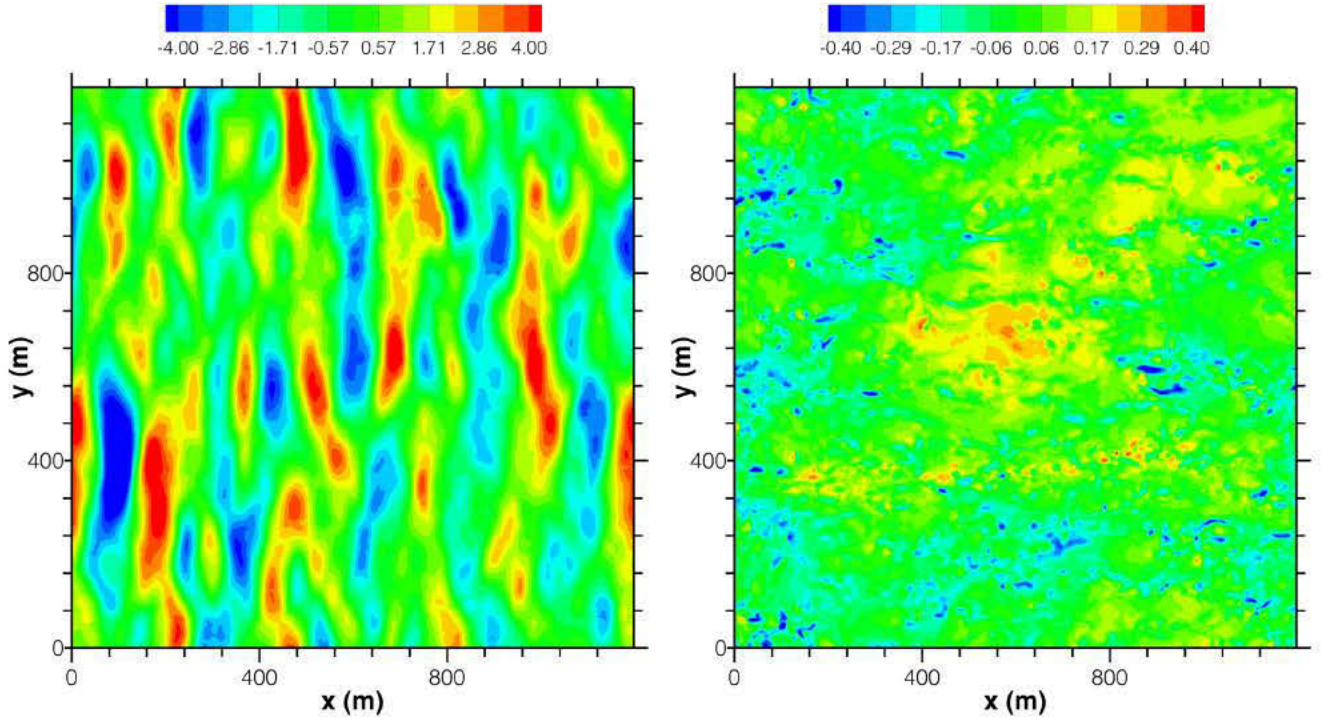


Figure 4: Static pressure fluctuations p'/ρ in sheared-convective flow over resolved waves (left panel) and over a flat surface (right panel) at a nominal height $\zeta = 5.8$ m. In the left panel the wave age $\mathcal{A} = C_p/U_{10} > 4$. Notice how the waves leave their imprint on flow in the surface layer. In each simulation the geostrophic wind $U_g = 5 \text{ m s}^{-1}$ and the surface heat flux $Q_* = 0.01 \text{ K m s}^{-1}$.

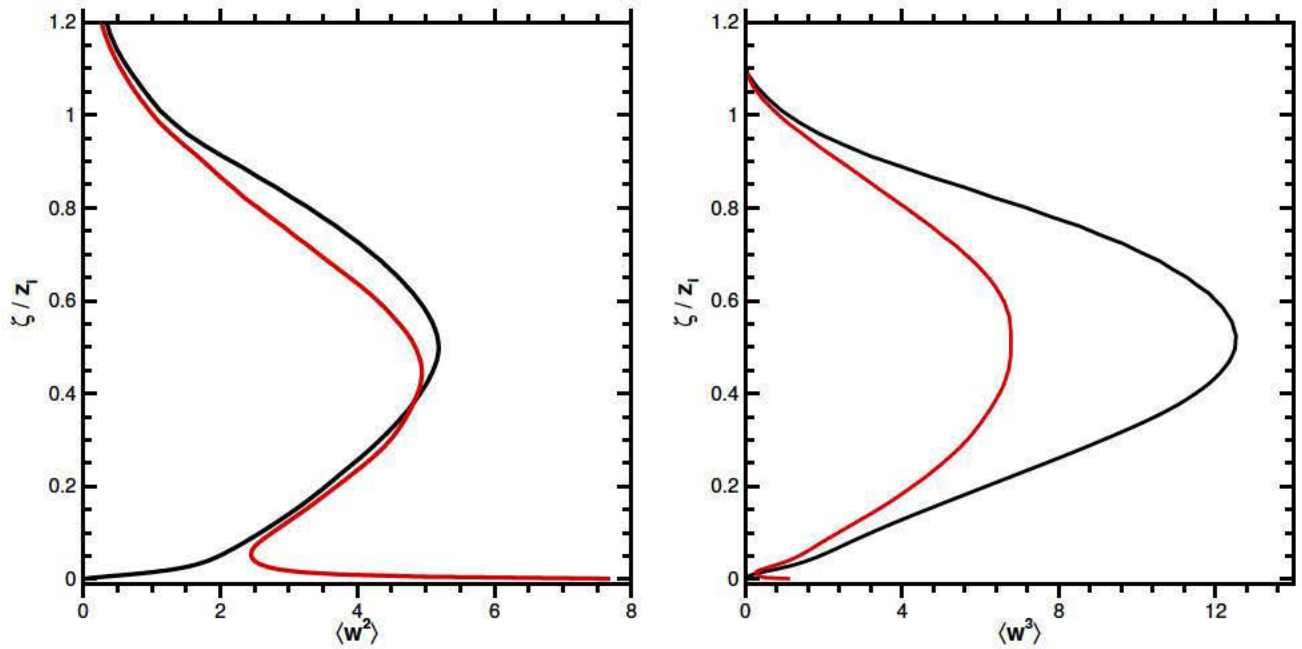


Figure 5: Vertical profiles of vertical velocity moments $\langle \bar{w}^2 \rangle / u_*^2$ (left panel) and $\langle \bar{w}^3 \rangle / u_*^3$ (right panel) for simulations over fast moving swell (red lines) and a smooth surface (black lines). The vertical coordinate ζ is made dimensionless by the boundary layer height z_i . Note the increased velocity variance induced by moving surface waves. The smaller value of the third order moment is evidence that surface waves have modified the vertical transport of turbulent kinetic energy in this sheared-convective boundary layer.